Lunar Reference Model Inferred From Gravity, Topography and Seismicity. Regan L. Patton, School of the Environment, Washington State University, Pullman, WA 99164-2812, rpatton@wsu.edu

Introduction: To what extent do global high-resolution gravity-topography spectra (Figure 1) reflect competent layering in the moon? This work examines the thermomechanical response of several competent layers, the lithosphere, tectosphere and mesosphere, based on the rock-like mechanics of differential grade-2 (DG2) materials [1].

Transitions in the size-morphology sequence of impact structures [2,3,4] are well-correlated with those predicted for a moon-sized sphere with a 194-km-thick lithosphere (Table 1). Focal depths for both deep and shallow moonquakes [5,6] and model pressures for multiply-saturated mare basalt sources [7] are consistent with this structure as well, suggesting that it might serve as a Lunar Reference Model (LuRM). Unexpected extremes in the lunar isotropy spectra, at degrees 2, 10, 11 and 12, reveal future opportunities for precise orbit determination, gravity and topography modeling and tidal displacement measurements.

Figure 1: Correlation (blue), admittance (green) and isotropy spectra (red) for high-resolution lunar gravity and topography models. Dashed vertical lines indicate transitional harmonics shown in Table 1. Stars denote unexpected extreme cross-covariance ratios.

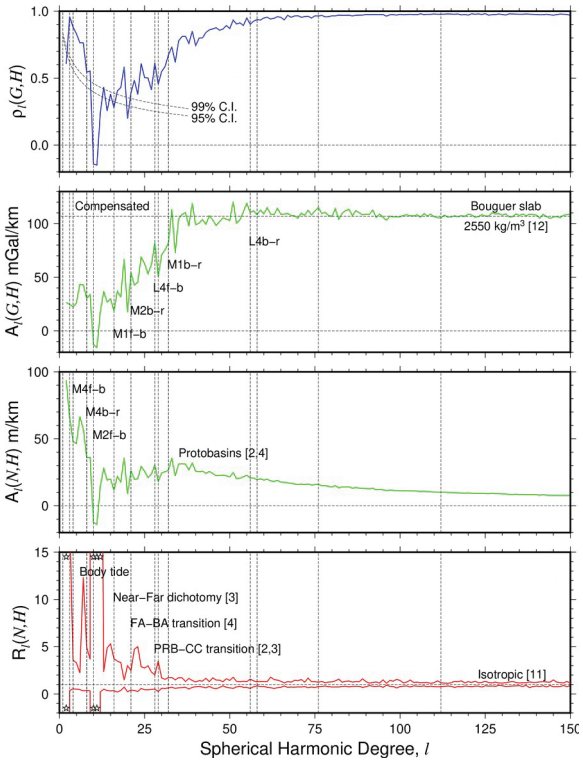

Global Spectra: Spectral statistics for potential model JGGRX1500E [8] and topography model LOLA2600P [9] were sampled at 40962 equally-spaced points on the lunar sphere. In what follows *G*, *H* and *N* denote spherical harmonic coefficients for gravity, topography, and the second-order selenoid, respectively (Figure 1).

As expected the degree correlation $\boldsymbol{\rho_l(G,H)}$ and admittances $\mathbf{A_l}(G,H)$ and $\mathbf{A_l}(N,H)$ are invariant under general rotations of the coordinate system. SHTOOLS [10] was used to compute these degree-wise estimates after each coordinate rotation. Interpretive methods for these measures based on classical isostatic and crustal thickness hypotheses are well-documented [9].

In contrast directional isotropy measures, like the cross-covariance ratio $\mathbf{R_l}(N,H)$ [11], are invariant only under rotations about the coordinate pole. Ratios close to unity indicate isotropy. By rotating the model fields with respect to the coordinate pole their directional dependence can be mapped. This variation is reflected in the spectra by the spread of values about unity, shown by plotting the maximum and minimum at each degree. Auto- and cross-covariance measures were computed using *ad hoc* Fortran code.

Table 1: LuRM layer thickness (z) and predicted weak-fold (w-f), fold-band (f-b), and band-rigid (b-r) transitional harmonics [1].

Layer	z (km)	w-f	f-b	b-r
H1	7.0	225	779	1559
H2	10.4	152	527	1054
H3	26.9	58	202	405
H4	28.0	56	194	389
L1	48.5	32	112	225
L2	71.7	21	76	152
L3	187	8	29	58
L4	194	8	28	56
M1	336	4	16	32
M2	497	3	10	21
M3	1292	1	4	8
M4	1344	1	4	8

Structural Theory: The structural theory of DG2 materials predicts a range of responses to loading depending on the thermomechanical competence (Figure 2). The leading order stress-energy balance is governed by a diharmonic equation [1].

In addition to the folding and faulting modes of deformation, which are well-expressed in Earth's gravity-topography spectra, the very-high energy

densities associated with hyper-velocity impact also activate fragmentation, equilibrium heating and distributed shearing in target rocks. Evidence for these higher energy modes is replete in the breccias, impact melts, and ejecta sampled by the Apollo, Luna and Chang'e missions [7].

Figure 2: Diharmonic structure diagram

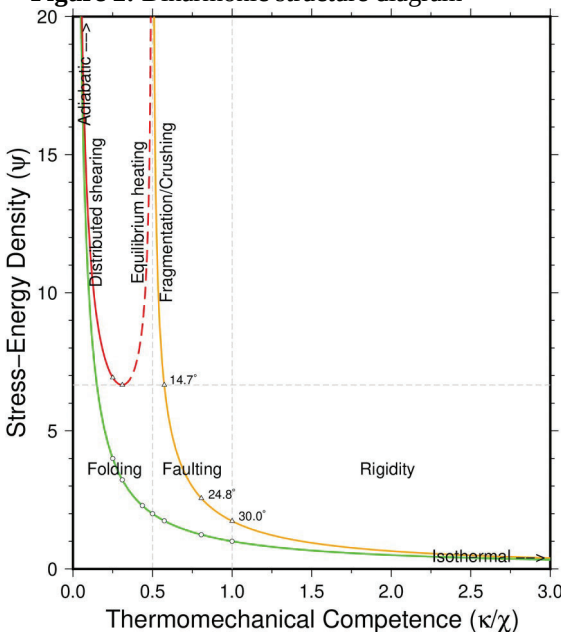

Interpretation: As shown in Figure 1, the correlation of lunar gravity and topography exceeds the 99% confidence limit at degrees 4-9, and for all degrees greater than 20 as well. In contrast, the correlation is less than the 95% confidence limit at degrees 2, 14, 16 and 20, and is negative at degrees 10 and 11. The latter degrees are often associated with mass concentrations [9] – free-air gravity highs over topographic basins [2,3,4]. Table 1 suggests that the lows at degrees 2, 10 and 20 are the result of diharmonic transitions in layer M2 (lower tectosphere).

Compared to a Bouguer slab model with crustal density 2550 kg/m^3 [12], lunar topography is compensated, to some extent, at all degrees less than about 35. The admittance decreases progressively down to degree 10, before increasing again at lower degrees. Table 1 suggests that compensation is the result of folding and faulting in layers L4, M1 and M2 (lithosphere and tectosphere), and at lower degrees by transitions in layer M4 (mesosphere). Protobasins [2,4] – impact structures featuring central peaks, like those in smaller complex craters, and peak-rings, common to larger basins – coincide with the spectral boundary between compensated and uncompensated lunar topography.

Isotropy spectra show that the moon is reasonably isotropic for all degrees greater than about 30. Anisotropy apparent at progressively lower degrees begins with the fold-band transition in the lithosphere (L4). This coincides with a morphometric [2] and gravitational [3] transition from peak-ring basins to complex craters as well.

Moonquakes occur in two depth ranges [5,6]. Shallow 'tectonic' events occur at depths of 50–220 km, coincident with the lithosphere (L4). Deep 'tidal' moonquakes occur mostly in the depth range 850-1000 km, coincident with the lower half of the mesosphere (M4).

Curiously, assuming wavelengths equal to deep moonquake depths, consistent with the band-rigid transition [1], deep events correspond to spherical harmonic degrees 10-12. This is where some of the unexpected extremes occur (Figure 1). Also note that the band-rigid transition in layer M4 is at degree 8, suggesting that the maximum at degree 7 is related to faulting in the mesosphere. Finally, given that maps of $\mathbf{R}_2(N,H)$ and $\mathbf{R}_7(N,H)$ are complementary to one another – lows in one match highs in the other, and *vice versa* – and the fact that tidal forcing is strongest at degree two, it seems likely that the unexpected extremes result from unmodeled or unmeasured time-dependent signals in lunar gravity and topography.

Acknowledgments: JGGRX1500E was obtained from the PDS Geosciences node. LOLA2600P was downloaded from author's website. Software used in this work includes SHTOOLS [10], GeographicLib [13] and the Generic Mapping Tools [14].

References: [1] Patton, R. L. and Watkinson, A.J (2019) *Geol. Soc. London Spec. Pub., 487,* 315-343. [2] Baker, D.M.H. *et al* (2011) *Icarus, 214,* 377-393. [3] Neumann, G.A. *et al* (2015) S*ci. Adv, 1,* e1500852. [4] Baker, D.M.H. *et al* (2017) *Icarus, 292,* 54-73. [5] Lammlein , D. R. *et al* (1974) *Rev. Geophys. Space Phys., 12(1),* 1-21. [6] Khan, A. *et al* (2000) *Geophys. Res. Lett., 27,* 1591-1594. [7] Wieczorek, M.A. *et al* (2006) *RIMG, 60,* 221-364. [8] Konopliv, A.S. *et al* (2014) *Geophys. Res. Lett., 41,* 1452-1458. [9] Wieczorek, M.A. (2015) *Treat. Geophys., 10.05,* 153-193. [10] Wieczorek, M.A. and Meschede, M. (2018) *Geochem. Geophys. Geosys., 19,* 2574-2592. [11] Bills, B.G. and Lemoine, F.G. (1995) *JGRE, 100,* 26275–26295. [12] Wieczorek, M.A, *et al* (2013) *Science, 339,* 671-674. [13] Karney, C.F.F. (2013) *J. Geod., 87,* 43-55. [14] Wessel, P. *et al* (2019) *Geochem. Geophys. Geosys., 20,* 5556-5564.